# Dielectric dispersion of short single-stranded DNA in aqueous solutions with and without added salt

Yoichi Katsumoto,* Shinji Omori, Daisuke Yamamoto, and Akio Yasuda
*Life Science Laboratory, Materials Laboratories, Sony Corporation, Sony Bioinformatics Center, Tokyo Medical and Dental University, Bunkyo-ku, Tokyo 113-8510, Japan*

Koji Asami
*Laboratory of Molecular Aggregation Analysis, Division of Multidisciplinary Chemistry, Institute for Chemical Research, Kyoto University, Uji, Kyoto 611-0011, Japan*

(Received 25 August 2006; published 16 January 2007; corrected 23 January 2007)

Dielectric spectroscopy measurements were performed for aqueous solutions of short single-stranded DNA with 30 to 120 bases of thymine over a frequency range of $10^5$ to $10^8$ Hz. Dielectric dispersion was found to include two relaxation processes in the ranges from $10^5$ to $10^6$ and from $10^6$ to $10^8$ Hz, respectively, with the latter mainly discussed in this study. The dielectric increment and the relaxation time of the high-frequency relaxation of DNA in solutions without added salt exhibited concentration and polymer-length dependences eventually identical to those for dilute polyion solutions described in previous studies. For solutions with added salt, on the other hand, those dielectric parameters were independent of salt concentration up to a certain critical value and started to decrease with further increasing salt concentration. This critical behavior is well explained by our newly extended cell model that takes into account the spatial distribution of loosely bound counterions around DNA molecules as a function of salt concentration.

DOI: 10.1103/PhysRevE.75.011911 PACS number(s): 87.15.He

## I. INTRODUCTION

Experimental proof by way of dielectric spectroscopy [1] and electric birefringence spectroscopy [2] is reliable for counterion polarization theories of polyelectrolytes [3,4] because of their straightforward principles and established methodologies. Here, it is quite important to characterize the ion atmosphere around polyelectrolytes without ambiguity of their molecular structure because the dielectric dispersion is affected by the dynamics of both the molecules and their ion atmospheres. Hence, the authors [5] conducted careful experiments for well-defined short double-stranded DNA (ds-DNA) which can be undoubtedly treated as straight polyions under experimental conditions commonly used and found that the scaling rules of the dielectric increment and the relaxation time as a function of polymer length cannot be accounted for by any theory so far proposed that gives analytical expressions for them. Since the previous study was performed only at a high salt concentration, we intend in this study to derive a broader physical picture about the dynamics of counterions around short DNA molecules over a wider range of salt concentration on the basis of more abundant experimental data.

A lot of past studies [1] show that the ion atmosphere around polyions (specifically DNA here) in aqueous solution consists of two portions, namely the condensed and diffused phases as briefly described below. Counterions diffuse and bind to the polyions from the surrounding electrolyte solution to reduce the strong Coulomb repulsion between the negatively charged phosphate groups, resulting in the formation of the condensed phase. Manning [6] showed that a large fraction of counterions condense onto the polyions to reduce the charge density if it exceeds a certain critical value, and the fraction is approximately 0.76 for ds-DNA in a monovalent-salt solution and is independent of salt concentration. Though these results are theoretically obtainable under very restricted conditions in which the polymer length diverges infinitely and the average spacing of the phosphate groups divided by the Debye screening length approaches zero in this order, they are experimentally verified under much more relaxed conditions [7]. In addition, the diffused phase of loosely bound counterions is formed surrounding the condensed phase in order to shield the charges of the residual phosphate groups.

The dielectric dispersion of a polyelectrolyte solution originates from the relaxation of the polarized ion atmosphere. There are two approaches to calculate important dielectric parameters such as dielectric increment and relaxation time. One is the analytical method to derive explicit expressions for those parameters, and the other is the numerical simulation. In one of the first approaches, the electrical polarizability is related to the time-correlation function of the dipole moment in the absence of the external electric field through the fluctuation-dissipation theorem [8], and the dielectric increment is calculated from the average of the square of the dipole moment resulting from thermal fluctuation of only the condensed counterions [9–11]. Another theoretical approach was discussed from the viewpoint of electro-optical techniques [12].

Fixman [13,14] employed a more direct but elaborate approach to solve the mutually coupled equations of motion for polyions, couterions and coions under the external electric field. Even though the theories take into account not only the condensed phase but also the diffused one, it still relies upon the "thin double-layer" approximation where the thickness of

*Electronic address: youichi.katsumoto@jp.sony.com

 

the ion atmosphere is small compared to the radius of curvature of the polyion. Rau and Charney [15] calculated the polarization of the diffused phase in the Debye-Hückel form without explicit use of the approximation about its thickness. These analytical approaches contain complicated mathematical techniques for solving nonlinear equations coupled with each other so that it is difficult to derive analytical solutions without rather extreme approximations not fully compatible with experimental conditions commonly used, though such solutions are valuable to understand the physical basis of the relaxation mechanism.

On the other hand, Washizu and Kikuchi [16,17] performed rigorous Metropolis Monte Carlo Brownian dynamics simulations for a 64 base-pair fragment of ds-DNA with salt concentrations from zero to 4.8 mM. Thus, their works are more compatible with our experiments and will be referred to in the following discussion. An obvious advantage of this approach at the expense of computational resource is its isolation from potential bias towards specific relaxation mechanisms or various ad hoc approximations. First, they confirmed that the ion atmosphere in an aqueous solution with added salt can be classified into two types of counterions in the condensed and diffused phases, just as qualitatively described so far. Secondly, they evaluated the relative importance of the two phases for the overall dipole moment by calculating the partial polarizability due to the first $n$ inner counterions, where $n$ is varied from unity to the total number of counterions, and pointed out that the loosely bound counterions in the diffused phase are dominant for the counterion polarization. This implies that the previous analytical theories, based on the consideration of only the condensed phase or on the thin double-layer approximation, would not be applicable to short polyelectrolytes as discussed in this article.

Turning to the experimental aspect, a difficulty in testing counterion theories of polyelectrolytes by means of dielectric spectroscopy is ascribable to the lack of sensitivity to detect the small dielectric increment for an extremely dilute solution in which the interaction among the polyions are negligibly small. Consequently, the intermolecular interactions are not avoidable and manifests as the solute concentration dependence of the dielectric dispersion. Ito *et al.* [18] performed dielectric spectroscopy measurements for sodium (polystyrene sulfonate) (NaPSS) solutions without added salt, which have different degrees of polymerization from 87 to 3800 with various solute concentrations. They concluded that the high-frequency relaxation is due to the polarization of loosely bound counterions in the diffused phase on the basis of the cell models [19] for both dilute and semidilute regions, where the characteristic length for the fluctuation of counterions $\xi$ is determined simply by the geometric consideration of the average distance between the neighboring polyions in water, which is equal to the correlation length [20] and is much smaller than the diameter of the diffused phase (note that the symbol $\xi$ is used for the characteristic length for counterions throughout this article, though it is used to present the correlation length in the referred literature). In a solution with added salt, however, since the thickness of the diffused phase changes as a function of salt concentration, the relative magnitude of the correlation length and the Debye screening length should be taken into account to determine $\xi$.

In summary of the previous studies, though it is quite clear from the results of the Monte Carlo simulation [16,17] that the diffused phase spatially extended outward plays a dominant role for the relaxation of short DNA solutions, the past theories only deal with the polarization of condensed counterions [9–11] or the polarization of loosely bound counterions with the thin double-layer approximation [13,14], and no systematic verification has been experimentally made for the effects of the spatial extent of the diffused phase.

Therefore, in this study we examine the influence of the spatial distribution of counterions on the dielectric properties of polyions, controlling the thickness of the ion atmosphere by systematically changing the solute and salt concentrations. Synthetic single-stranded DNA (ss-DNA) was used for this purpose because its degree of polymerization can be controlled precisely by solid-phase synthesis. If ds-DNA were selected as in our previous work [5] for such experiments, uncertainties would be higher because the chemical equilibrium of the hybridization reaction should be taken into account for each salt concentration, especially for a low salt concentration where ds-DNA can be partially denatured into its complementary strands. It might be seen at first sight that structural uncertainty is enhanced when less rigid ss-DNA is used, but this is not the case because use of oligodeoxythymidylates as mentioned in the next section allows simple wormlike chain modeling [21].

## II. EXPERIMENT

To exclude uncertainties associated with the polymer-length distribution inherent to specimens with biological origin used for the past studies, synthetic DNA with lengths of 30, 59, 90, and 120 bases (Operon Biotechnologies, Inc.) was used. The specimens are composed of only thymine among the four possible bases to avoid the formation of intramolecular structure that can be confusing for the interpretation of the experimental data. The high-performance liquid chromatography (Waters 600, Waters) or the time-of-flight mass spectrometer (Axima-LNR, Shimadzu) was used to confirm that each specimen virtually has a unique molecular weight. First, freeze-dried specimens as received were dissolved in doubly deionized water. Secondly, the initial concentrations were determined from the absorbance of ultraviolet light at a wavelength of 260 nm, and then the solutions were diluted with water to the final weight concentrations $C_w$ of 0.25, 0.50, 1.0, and 2.0 g/l.

In order to reduce experimental errors due to the variation of $C_w$ among the specimens with different NaCl concentrations $C_s$ from 0.0 to 30 mM at a constant nominal $C_w$, the same specimen was used throughout a series of measurements for a constant nominal $C_w$ by adding a small amount of concentrated NaCl solution to increase $C_s$ in a stepwise way. The estimated error in $C_w$ induced by such stepwise dilution is approximately 0.5% for a single step and less than 3% between the initial and final solutions, which does not affect the discussion about the $C_w$ dependence of the dielectric parameters in Sec. III.

An impedance analyzer (4294A, Agilent Technologies) was used for dielectric measurement. A capacitor-type cell

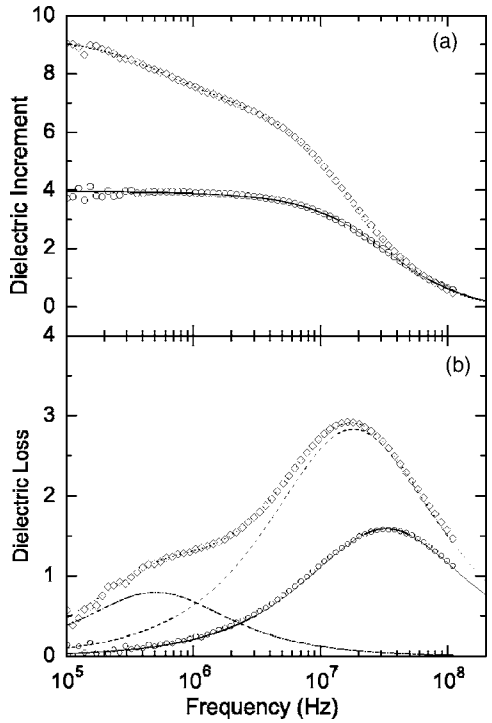


FIG. 1. The real (a) and imaginary (b) parts of the complex dielectric constants for salt-free ss-DNA solutions with the length of 30 (○) and 120 (◇) bases at the weight concentration of 1.0 g/l. The solid and dotted curves for the real and imaginary parts are theoretical curves calculated from one or two Cole-Cole functions with the fitted parameters for 30 and 120 bases, respectively. The loss spectrum for 120 bases in (b) can be decomposed into dash-dotted and dashed curves corresponding to low- and high-frequency relaxations, respectively.

made of acrylic resin has two parallel platinum electrodes with the spacing of 3.5 mm and the diameter of 8 mm, which were carefully plated with platinum black to reduce electrode-polarization effects. The temperature of the sample solution was maintained at 298±0.1 K by circulating water around the cell. Measurements were performed over the frequency range from 40 to $1.1\times10^8$ Hz with the applied peak-to-peak voltage of 0.30 V.

The evaluation of the cell constant and the calibration of the residual inductance and the parasitic capacitance over the whole circuitry were performed according to the method described elsewhere [22]. The complex dielectric constants and dc conductivities were measured for solvents with $C_s$ =0.10–50 mM, and the complex dielectric constant for a hypothetical solvent that has the same dc conductivity as the sample DNA solution was derived by interpolation and subtracted from that of the sample solution to yield the complex dielectric increment $\Delta\epsilon^*$ with the correction of electrode-polarization effects automatically implemented.

## III. RESULTS AND DISCUSSION

### A. Quantitative analysis of dielectric dispersion

The dielectric dispersions for ss-DNA with 30 and 120 bases at $C_w$=1.0 g/l in water are shown in Fig. 1. Low- and high-frequency dielectric loss peaks around $5\times10^5$ and $2\times10^7$ Hz, respectively, can be clearly seen for 120-base ss-DNA in Fig. 1(b), while only a single peak can be seen for 30-base ss-DNA probably because the other is vanishingly small. Thus, fitting was performed with the assumption that $\Delta\epsilon^*$ is represented as the superposition of two Cole-Cole functions as follows, though one of them was neglected for the cases where the separation of the two dielectric loss peaks is small or one of them is relatively small compared to the other:

$$\Delta\epsilon^*(\omega)=\frac{\Delta\epsilon_L}{1+(i\omega\tau_L)^{\beta_L}}+\frac{\Delta\epsilon}{1+(i\omega\tau)^{\beta}}+\Delta\epsilon_\infty, \qquad (1)$$

where $i=\sqrt{-1}$, $\omega=2\pi f$, $f$ is the frequency, $\Delta\epsilon_\infty$ is the difference of the dielectric constants between the tested sample and the referred hypothetical solvent in the high frequency limit of $f\to\infty$, and the sets of parameters $(\Delta\epsilon_L,\tau_L,\beta_L)$ and $(\Delta\epsilon,\tau,\beta)$ are the dielectric increments, relaxation times and Cole-Cole parameters for the low- and high-frequency relaxations, respectively.

Two relaxations were clearly observed for 59-, 90-, and 120-base ss-DNA in water, though only the data for 120-base ss-DNA are presented in Fig. 1. The dielectric increments and relaxation times of these two relaxations, together with those of one relaxation for 30-base ss-DNA, as obtained by using Eq. (1) are plotted against the degree of polymerization $N$ at $C_w$=1.0 g/l in Fig. 2. It is seen that both $\Delta\epsilon_L$ and $\tau_L$ are approximately proportional to $N^2$, while both $\Delta\epsilon$ and $\tau$ are approximately proportional to $N^{2/3}$. The $N^2$ dependences of $\Delta\epsilon_L$ and $\tau_L$ were also observed by Takashima [23] for much longer DNA and are fairly consistent with the prediction of the counterion condensation theories [9–11,24,25], so that the low-frequency dispersion is due to the relaxation of the condensed phase. On the other hand, the $N^{2/3}$ dependences of $\Delta\epsilon$ and $\tau$ were also observed by Ito *et al.* [18] for NaPSS in the dilute region and are discussed in more detail in Sec. III B. Since $\Delta\epsilon$ and $\tau$ are expected to be independent of $N$ in the semidilute region, all the specimens used in this study can be treated as dilute solutions.

The $N^2$ dependence of $\tau_L$ makes the numerical deconvolution of the two relaxations more difficult as $N$ decreases because the difference between $\tau_L$ and $\tau$ decreases as shown in Fig. 2(b). Fortunately, since the ratio $\Delta\epsilon_L/\Delta\epsilon$ also decreases down to 0.03 at $N$=30 as expected from Fig. 2(a), the low-frequency relaxation is negligible for 30-base ss-DNA, even though the numerical deconvolution cannot be performed. Therefore, we employ the data for the solutions of ss-DNA with all the polymer lengths of $N$=30, 59, 90, and 120 when discussing the $C_w$ dependence of the high-frequency relaxations in aqueous solutions without salt in Sec. III B.

On the other hand, as $C_s$ increases, the low-frequency dispersion is gradually affected by the electrode-polarization effects. This can be seen in the dielectric dispersions for ss-DNA with 30 bases at $C_w$=1.0 g/l with variable $C_s$ shown in Fig. 3. In addition, since $\tau$ increases with increasing $C_s$ as can be qualitatively seen for 30-base ss-DNA in Fig. 3, the separation of the two relaxations becomes difficult for higher

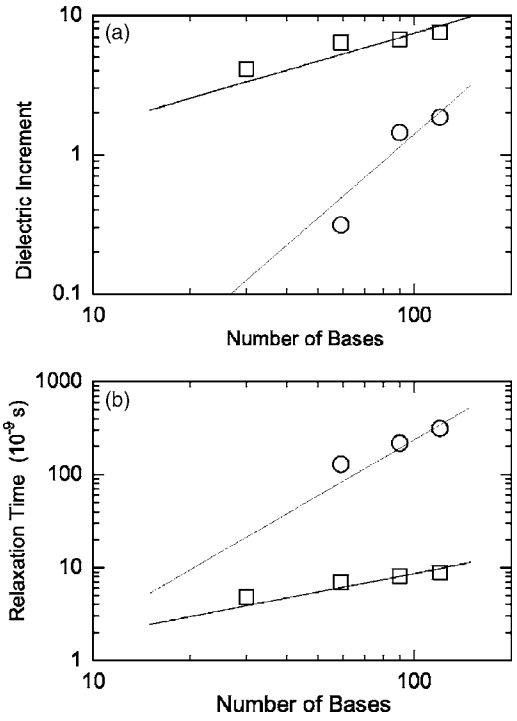


FIG. 2. The dielectric increments (a) and the relaxation times (b) of low- and high-frequency relaxations (○ and □, respectively) as a function of base number at the weight concentration of 1.0 g/l in double logarithmic plots. The solid lines are the least-square fits to the experimental data with the fixed gradients of 2 and 2/3 for the low- and high-frequency relaxations, respectively, and the correlation coefficients are 0.940 and 0.943 for $\Delta\epsilon_L$ and $\Delta\epsilon$, and 0.888 and 0.839 for $\tau_L$ and $\tau$, respectively (see the text for the symbol definition).

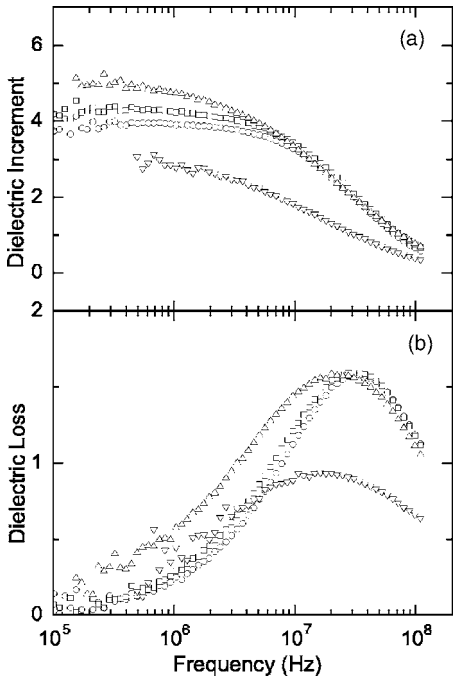


FIG. 3. The real (a) and imaginary (b) parts of the complex dielectric constants for 30-base ss-DNA solutions with the salt concentrations of 0.0 (○), 0.30 (□), 3.0 (△), and 30 (▽) mM at the weight concentration of 1.0 g/l.

$C_s$. Thus, we focus only on 30- and 59-base ss-DNA for which the high-frequency relaxation is obviously dominant as shown in Fig. 2(a) and the low-frequency relaxation can be safely neglected even if the numerical deconvolution cannot be performed, when discussing the $C_s$ dependence of the high-frequency relaxations in aqueous solutions with salt in Sec. III C. On the other hand, we do not discuss 90- and 120-base ss-DNA because the low-frequency relaxation inseparable from the higher one at high $C_s$ cannot be ignored in contrast to 30- and 59-base ss-DNA.

### B. Aqueous solution without salt

As mentioned in the previous section, the dependences of $\Delta\epsilon$ and $\tau$ on $N$ implies that all the ss-DNA solutions in water used for this study are dilute. Therefore, the correlation length (the average distance between the neighboring polyions) is larger than the polymer length $L$. Ito *et al.* [18] estimated $\tau$ in the dilute region as follows. The electrostatic potential exerted on counterions around a polyion has the spatial periodicity of the correlation length, which is equal to the characteristic length for the fluctuation of counterions $\xi$ and depends on $C_w$ through the number concentration $n_p$ in Eq. (2),

$$\xi \sim n_p^{-1/3}, \tag{2}$$

where $n_p \propto C_w/N$. It should be noted that $\xi$ is not characterized by the Debye screening length $\kappa^{-1}$. The ion atmosphere around the central polyion is eventually isotropic unless $\xi \leq L$. Since loosely bound counterions in the diffused phase fluctuate in the potential well defined by $\xi$, the relaxation time is given by

$$\tau \sim \frac{\xi^2}{2D} \propto \xi^2 \propto C_w^{-2/3} N^{2/3}, \tag{3}$$

where $D$ is the diffusion constant of counterions. In Fig. 4, $\tau$

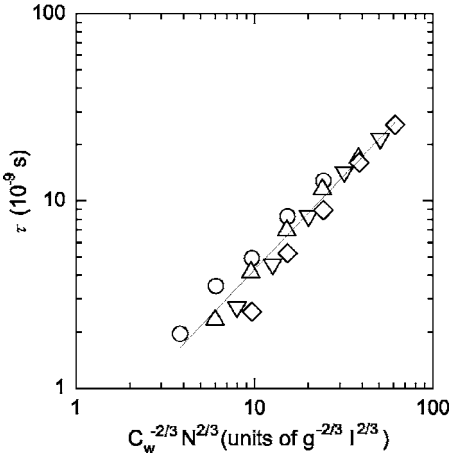


FIG. 4. The relaxation time $\tau$ for ss-DNA with $N$=30 (○), 59 (△), 90 (▽), and 120 (◇) bases in solution without salt as a function of $C_w^{-2/3} N^{2/3}$ for all the weight concentrations $C_w$ employed in the experiments in a double logarithmic plot. The solid line is the least-square fit to the experimental data with the gradient of unity, and the correlation coefficient is 0.988.

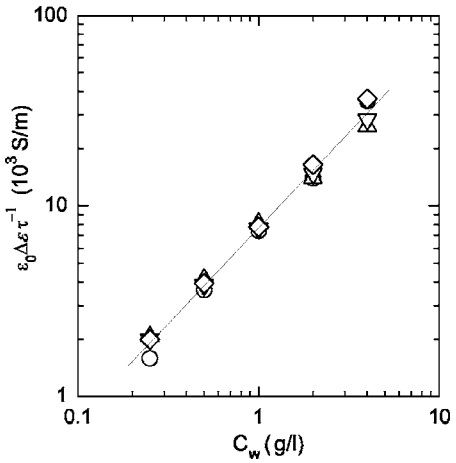


FIG. 5. The quantity $\epsilon_0\Delta\epsilon/\tau$ proportional to the number of counterions associated with a single polyion (see the text) for ss-DNA with 30 (○), 59 (△), 90 (▽), and 120 (◇) bases in solution without salt as a function of weight concentration $C_w$ in a double logarithmic plot. The solid line is the least-square fit to the experimental data with the gradient of unity, and the correlation coefficient is 0.996.

for ss-DNA solutions without salt is plotted as a function of $C_w^{-2/3}N^{2/3}$. It is seen that Eq. (3) fits the experimental data quite well with the correlation coefficient of 0.988.

The same model also gives $\Delta\epsilon$ as

$$\Delta\epsilon \sim \frac{n_c e^2 \xi^2}{\epsilon_0 k_B T} \propto n_c \xi^2, \tag{4}$$

where $n_c$ is the number of counterions in the diffused phase associated with a single polyion, and $e$, $k_B$, $T$, and $\epsilon_0$ are the elementary charge, the Boltzmann constant, the temperature, and the dielectric constant, respectively. From Eqs. (3) and (4), $n_c$ is related to $\tau$ and $\Delta\epsilon$ as

$$n_c \propto \frac{\Delta\epsilon}{\tau}. \tag{5}$$

Theoretical calculations [26,27] showed that $n_c$ is proportional to $C_w$ in the semidilute region, and Ito *et al.* [18] revealed experimentally for NaPSS solutions without salt that this proportionality is also valid in the dilute region. In Fig. 5, $\epsilon_0\Delta\epsilon/\tau$ for ss-DNA solutions without salt is plotted against $C_w$ and is linearly fitted with the correlation coefficient of 0.996, which indicates that the relation

$$n_c \propto C_w \tag{6}$$

is well satisfied for short ss-DNA solutions, just as for NaPSS solutions.

Therefore, from Eqs. (3), (5), and (6), the following relation of $\Delta\epsilon$ to $C_w$ and $N$ has been established for short ss-DNA solutions

$$\Delta\epsilon \propto C_w^{1/3} N^{2/3}. \tag{7}$$

In summary of this section, the polarization of loosely bound counterions, which are distributed in the periodic electrostatic potential defined by $\xi$ related to $C_w$, is dominant for the high-frequency relaxation of a short ss-DNA solution without salt. Since all the experimental data were well described by the model for the dilute region, the model is extended only for the dilute region in the next section.

### C. Aqueous solution with salt

Use of the cell model developed in Sec. III B is limited to the salt-free or low-salt condition where the diameter of the diffused phase proportional to $\kappa^{-1}$ given below is much larger than the correlation length given by Eq.(2):

$$\kappa^{-1} = \left(\frac{\epsilon k_B T}{2N_A e^2 I}\right)^{1/2}, \tag{8}$$

where $\epsilon$ is the permittivity of water, $N_A$ is the Avogadro's number, and $I$ is the ionic strength of the solution ($I=C_s$ for monovalent salt). However, as shown below, the model can be further extended for solutions with added salt if the distribution of counterions is appropriately considered. Since, as demonstrated so far, the relevant relaxation here is mainly due to the fluctuation of loosely bound counterions, the diameter of the diffused phase as a function of $C_s$ is critical.

In an aqueous solution without salt, as discussed in Sec. III B, $\xi$ is of the same order of magnitude as the size of the cell which a polyion occupies exclusively in the dilute region [see Eq. (2)]. On the other hand, the diameter of the diffused phase is of the same order of magnitude as $\kappa^{-1}$ multiplied by a constant explained just below and is much larger than $n_p^{-1/3}$ in water or in a solution at very low $C_s$. As $C_s$ increases, the diameter decreases while $n_p^{-1/3}$ remains constant, and they equate at a certain critical concentration $C_s^*$. With further increasing $C_s$, the diameter of the diffused phase is determined by the spatial extent of the Debye-Hückel potential instead of $n_p^{-1/3}$. The idea is depicted in Fig. 6.

It is well known for a small ion that the Debye screening length $\kappa^{-1}$ is the radius with respect to the central ion, at which the existing probability of a counterion to shield the central charge has its maximum. For a polyion, on the other hand, counterions in the diffused phase should feel a weaker potential of the central polyion than the one calculated from the simple Debye-Hückel approximation because of the counterion condensation as mentioned in the Introduction. Thus, it is obvious that some scale factor must be used to define the boundary of the ion atmosphere, though it might not be given in a simple form.

For the high-salt condition, therefore, we adopt $2c\kappa^{-1}$ instead of $n_p^{-1/3}$ for $\xi$ where $c$ is the proportional constant. According to the Monte Carlo simulation study for a 64 base-pair fragment of ds-DNA [28], the $n$th net charge in the distribution of counterions and coions has the maximum probability density at the radial distance of approximately $4\kappa^{-1}$ from the polyion regardless of $C_s$, where $n$ is the number of the phosphate groups (128 for the example here). We use this definition for the boundary of the ion atmosphere and set $c=4$ accordingly throughout the following discussion, because there were no other sources available for experimental conditions close if not identical to ours.

Prior to further formulation, it should be noted that the persistence length $l_p$ of the polyion is another important pa-

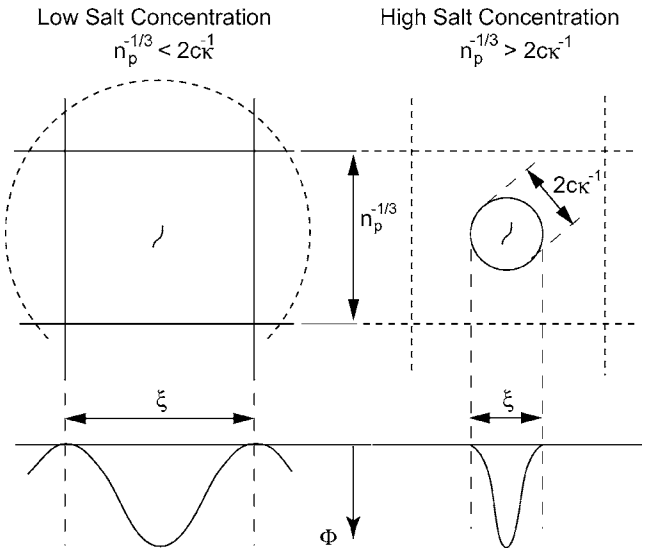


FIG. 6. Schematic of the proposed cell model. The extent of the diffused phase around a single polyion in the center, where loosely bound counterions are distributed within the electrostatic potential well of Φ, is shown as the solid lines. The characteristic length for the counterion fluctuation $\xi$ is equal to the side length of the cubic cell in which a polyion occupies exclusively at a low salt concentration (the left-hand side) and the diameter of the diffused phase $2c\kappa^{-1}$ at a high salt concentration (the right-hand side), respectively, where $\kappa^{-1}$ is the Debye screening length and $c$ is the proportional constant (see the text for the detail).

rameter which is related to the stiffness of the polyion for the model depicted in Fig. 6. If $\xi=2c\kappa^{-1}$ is smaller than the polymer length $L$ (the end-to-end distance of the polyion), the ion atmosphere around the polyion is highly anisotropic, and so is its polarization. Therefore, two relaxations in the longitudinal and transversal directions with respect to the polyion must be taken into account separately. In fact, such consideration may be required for longer ss-DNA with, say, 90 and 120 bases not discussed in this section for the reason addressed in the end of Sec. III A. On the other hand, as shown just below, the anisotropy of the ion atmosphere is not critical in analyzing the data for 30- and 59-base ss-DNA.

Since $\kappa^{-1}$ is inversely proportional to $C_s^{1/2}$ [see Eq. (8)] and the minimum value in this study is 1.8 nm at $C_s=30$ mM, $2c\kappa^{-1}$ is 14.4 nm at $C_s=30$ mM with $c=4$ and increases as $C_s$ decreases. On the other hand, a fluorescence resonance energy transfer study [21] indicates that $l_p$ is approximately 3 nm for ss-DNA of 10 to 70 thymines at $C_s=25$ mM, and the polymer length $L$, estimated as $l_p(Nb/l_p)^{1/2}$ on the basis of the simplest wormlike chain model, are 7.5 and 10.6 nm for ss-DNA with 30 and 59 bases, respectively, where $b$ is the average spacing of the phosphate groups and set to be 0.63 nm [21]. Thus, the ion atmosphere can be treated as rather isotropic even at 30 mM.

Among theories about the persistence length of polyelectrolytes [21,29,30], the early theories of Odijk [31] and Skolnick and Fixman [32] predict that $l_p$ is given as the sum of the constant part and the variable part proportional to the inverse of ionic strength. Therefore, as $C_s$ decreases, $l_p$ increases and levels off at a certain point where $l_p$ reaches the size of the electrostatic blobs, approximately 3 nm for ss-DNA in water [see Eq. (43) of Ref. [1]]. On the other hand, $2c\kappa^{-1}$ continues to increases as $C_s$ decreases. Thus, it is confirmed that the diameter of the ion atmosphere is greater than the polymer length over all the salt concentration range in this study.

In summary, $\xi$ is expressed as

$$\xi \sim n_p^{-1/3} \text{ (dilute region, low salt concentration, } 2c\kappa^{-1} > n_p^{-1/3} > L), \tag{9}$$

$$\xi \sim 2c\kappa^{-1} \text{ (dilute region, high salt concentration } n_p^{-1/3} > 2c\kappa^{-1} > L). \tag{10}$$

Thus, by referring to Eqs. (3), (4), and (6) $\Delta\epsilon$ and $\tau$ follow the scaling rules below:

$$\Delta\epsilon \propto n_c(n_p^{-1/3})^2 \propto C_w^{1/3}N^{2/3}I^0 \quad \text{(dilute region, low salt concentration)}, \tag{11}$$

$$\Delta\epsilon \propto n_c(2c\kappa^{-1})^2 \propto I^{-1} \quad \text{(dilute region, high salt concentration)}, \tag{12}$$

$$\tau \propto (n_p^{-1/3})^2/2D \propto C_w^{-2/3}N^{2/3}I^0 \quad \text{(dilute region, low salt concentration)}, \tag{13}$$

$$\tau \propto (2c\kappa^{-1})^2/2D \propto I^{-1} \quad \text{(dilute region, high salt concentration)}. \tag{14}$$

At the crossover point of low and high salt concentrations, the following equation should hold:

$$2c\kappa^{-1} = n_p^{-1/3}. \tag{15}$$

Then, the critical ionic strength $I^*$ (equals to $C_s^*$ for monovalent salt) is given by

$$I^* = 2c^2\frac{\epsilon k_B T C_w^{2/3}}{N_A^{1/3}e^2M_w^{2/3}}, \tag{16}$$

where $M_w$ is the molecular weight of the polyion. Finally, from the continuity of $\Delta\epsilon$ and $\tau$ across $I^*$, we obtain

$$\Delta\epsilon = AC_w^{1/3}N^{2/3}I^0 \tag{17}$$

and

$$\tau = BC_w^{-2/3}N^{2/3}I^0 \tag{18}$$

for $I<I^*$, and

$$\Delta\epsilon = AC_w^{1/3}N^{2/3}\frac{I^*}{I} = 2Ac^2\frac{\epsilon k_B T}{N_A^{1/3}e^2}C_w\left(\frac{N}{M_w}\right)^{2/3}I^{-1} = 2A\frac{c^2}{m^{2/3}}\frac{\epsilon k_B T}{N_A^{1/3}e^2}C_w^1N^0I^{-1} \tag{19}$$

and

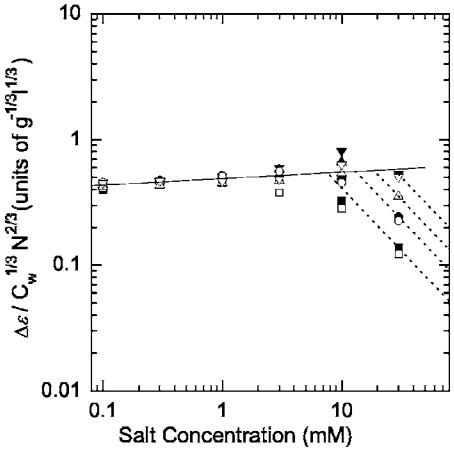


FIG. 7. The normalized dielectric increment $\Delta\epsilon/C_w^{1/3}N^{2/3}$ for ss-DNA with $N=30$ (open symbols) and 59 (filled symbols) bases in solution with the weight concentrations $C_w$ of 0.25 (□), 0.50 (○), 1.0 (△), and 2.0 (▽) g/l as a function of salt concentration $C_s$ in a double logarithmic plot. The solid line is the regression line to the experimental data for $C_s$ from 0.10 to 1.0 mM, and each dotted line has a negative unity gradient and passes through the data point for 30-base ss-DNA at $C_s=30$ mM. The increment remains almost constant but slightly increases with increasing $C_s$ below 1 mM and decreases along the dotted lines. The salt concentrations at the crossover points of the solid and dotted lines agree well with the critical salt concentrations as calculated by $2c\kappa^{-1}=n_p^{-1/3}$ (see the text).

$$\tau = BC_w^{-2/3}N^{2/3}\frac{I^*}{I} = 2B\frac{c^2}{m^{2/3}}\frac{\epsilon k_B T}{N_A^{1/3}e^2}C_w^0 N^0 I^{-1} \qquad (20)$$

for $I>I^*$, where $m$ is the molecular weight of the monomer, and $A$ and $B$ are constants.

In Fig. 7, $\Delta\epsilon$ normalized by $C_w^{1/3}N^{2/3}$ according to Eq. (17) for ss-DNA with 30 and 59 bases at various $C_w$ are shown in a double logarithmic plot as a function of $C_s$. The solid line is a regression line to all the experimental data within the range of $C_s=0.1-1$ mM. Such good fit with a small gradient means that $\Delta\epsilon/C_w^{1/3}N^{2/3}$ is almost constant below $C_s=1$ mM, and our model for the free-salt condition described in Sec. III B explains well the high-frequency relaxation with not only $C_s=0$ but also low $C_s$ as implied by Eq. (17). The four dotted lines, corresponding to the four $C_w$, with negative unity gradients that pass through the data points for 30-base ss-DNA at $C_s=30$ mM were drawn according to Eq. (19) where $\Delta\epsilon$ is shown to be inversely proportional to $I$ for $I>I^*$, and the data are consistent with the expectation though the limited number of data points in the high-salt region prevents complete confirmation. Unfortunately, we were unable to acquire the reliable data neither for more than $C_s=30$ mM nor for less than $C_w=0.25$ g/l because $\Delta\epsilon$ becomes so small that increasing noises from the electrode-polarization effects prevent accurate quantification. To overcome this problem, serious consideration of the correction for the effects [33] are required to extend the measurable region of $C_s$.

In order to further investigate the agreement of the proposed model with the experimental results, we calculated the critical salt concentrations $C_s^*$ for 30- and 59-base ss-DNA using Eq. (16) and compared them to the experimental data which were obtained as the crossover points of the solid and dashed lines in Fig. 7. Results are summarized in Table I.

TABLE I. Critical salt concentrations $C_s^*$ calculated by Eq. (16) and those calculated from the experimental results for the 30- and 59-base ss-DNA solutions with added salt.

| $C_w$ [g/l] | | 0.25 | 0.50 | 1.0 | 2.0 |
|---|---|---|---|---|---|
| Theoretical $C_s^*$ [mM] | 30 bases | 9.8 | 16 | 25 | 39 |
| | 59 bases | 6.3 | 9.9 | 16 | 25 |
| Experimental $C_s^*$ [mM] | 30 bases | 7.6 | 13.1 | 18.6 | 27.4 |
| | 59 bases | 6.8 | 12.2 | 18.6 | 26.2 |

A series of $C_s^*$ calculated by Eq. (16) agree relatively well with those calculated from the experimental results, supporting the claim that the critical behavior as observed in Fig. 7 is due to the transition of the characteristic length for counterion fluctuation as depicted in Fig. 6.

The normalized relaxation time $\tau/C_w^{-2/3}N^{2/3}$ according to Eq. (18) for ss-DNA with 30 and 59 bases at various $C_w$ are shown in a double logarithmic plot as a function of $C_s$ in Fig. 8. As expected from Eqs. (18) and (20), it remains almost constant until $C_s$ reaches $C_s^*$ and decreases in an inversely proportional way to $C_s$ when $C_s>C_s^*$. The dependence of $\tau$ is qualitatively well explained by our model, but the agreement between experiment and theory is not as good as that for $\Delta\epsilon$ in Fig. 7, because the normalized $\tau$ gradually increases when $C_s<C_s^*$ in contrast to the prediction from Eq. (18). This is probably due to the following reason. While $\Delta\epsilon$ can be derived from the thermal fluctuation of counterions without the external electric field through the fluctuation-dissipation theorem as mentioned in Sec. I, the diffusional relaxation mechanism for loosely bound counterions needs to be considered for more accurately analyzing $\tau$. Our model agrees well with experiment for aqueous solutions without salt

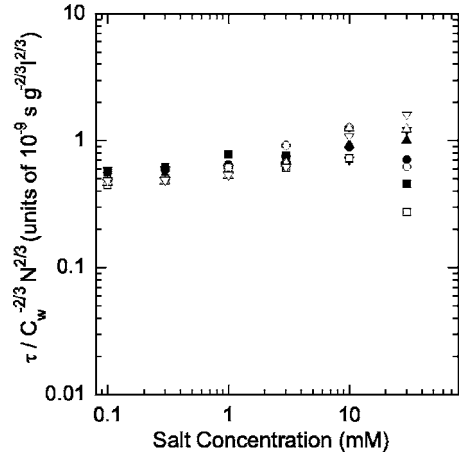


FIG. 8. The normalized relaxation time $\tau/C_w^{-2/3}N^{2/3}$ for ss-DNA with $N=30$ (open symbols) and 59 (filled symbols) bases in solution with the weight concentrations $C_w$ of 0.25 (□), 0.50 (○), 1.0 (△), and 2.0 (▽) g/l as a function of salt concentration $C_s$ in a double logarithmic plot.

where $2c\kappa^{-1}$ is much larger than the cell size and the diffusion constant $D$ inside the cell remains nearly constant. On the other hand, the dependence of $D$ on position in the diffused phase must be considered when the theory is extended to the case where $2c\kappa^{-1}$ changes gradually as a function of $C_s$. That is, $D$ for loosely bound counterions decreases as $2c\kappa^{-1}$ decreases, because the electrostatic attractive forces from the phosphate groups increase to hinder the movement of the counterions as they approach the polyion.

In fact, early polarization theories of colloidal solutions [34,35] use the surface conductivity as the overall contribution from counterions having different mobilities as a function of distance from the polyion; the mobility in the inner layers is several times smaller than that in the outer layers because of the electrostatic attractive forces. Referring to this consideration that $D$ for loosely bound counterions decreases and approaches that for condensed counterions as $C_s$ increase, the normalized $\tau$ is expected to increase as a function of $C_s$, and the results shown in Fig. 8 are fairly consistent with this argument.

Finally, we briefly mention the application of the model to our previous experimental results concerning the dielectric relaxations of short ds-DNA solutions at $C_s=30$ mM [5]. Since the persistence length of short ds-DNA with 120 base pairs is greater than 50 nm [36], the polymer length $L$ is likely to be almost identical to its contour length, approximately 40 nm for 120 base-pair ds-DNA, while $2c\kappa^{-1}$ is 14 nm as mentioned above. In this case, it is obvious that the anisotropy of the ion atmosphere should be taken into account. Nevertheless, our model can be further extended in such a way that the longitudinal and transversal fluctuation lengths, $\xi_{\parallel}$ and $\xi_{\perp}$, along the major and minor axes of ds-DNA, respectively, are defined and set to be $2c\kappa^{-1}+L$ and $2c\kappa^{-1}$, respectively. Numerical simulation shows that the two relaxations are too close to be separately observed at $C_s=30$ mM and the superposition of them can explain the anomalous scaling rules of $\Delta\epsilon$ and $\tau$ as a function of $N$ as observed in Ref. [5]. Since the analysis for ss-DNA with relatively long polymer lengths of $N=90$ and 120 with added salt has not been performed in this article for the reason described in Sec. III A, it will be presented elsewhere together with the numerical simulations for ds-DNA, on the basis of the anisotropic model briefly suggested here.

## IV. CONCLUSIONS

In this work, first we showed that the high-frequency relaxations of short ss-DNA solutions without added salt exhibited the concentration and polymer-length dependences eventually identical to those for dilute solutions of polyions such as NaPSS reported in the previous studies, and the same dependences were also established for solutions with salt concentrations lower than a certain critical value.

Secondly, it was shown that the polarization of loosely bound counterions is dominant for the high-frequency relaxation, and its dielectric dispersion is well explained by the cell model where the counterions fluctuate in the periodic electrostatic potential defined by the correlation length as a function of solute concentration in the dilute region.

Thirdly, on the other hand, for solutions with added salt, the dielectric increment and the relaxation time were almost independent of salt concentration up to the critical value and started to decrease with further increasing salt concentrations. More specifically, they are inversely proportional to the ionic strength above the critical salt concentration. Finally, this critical behavior is explained by our extended cell model that takes into account the spatial extent of the diffused phase as a function of salt concentration and utilizes it instead of the correlation length for the characteristic length of the counterion fluctuation.

## ACKNOWLEDGMENTS

The authors thank Dr. Y. Hayashi for his careful reading of the paper.

[1] F. Bordi, C. Cametti, and R. H. Colby, J. Phys.: Condens. Matter **16**, R1423 (2004).
[2] Y. Lu, B. Weers, and N. C. Stellwagen, Biopolymers **61**, 261 (2002).
[3] F. Oosawa, *Polyelectrolytes* (Marcel Dekker, New York, 1971).
[4] M. Mandel and T. Odjik, Annu. Rev. Phys. Chem. **35**, 75 (1984).
[5] S. Omori, Y. Katsumoto, A. Yasuda, and K. Asami, Phys. Rev. E **73**, 050901 (2006).
[6] G. S. Manning, Q. Rev. Biophys. **11**, 179 (1969).
[7] M. O. Fenley, G. S. Manning, and W. K. Olson, Biopolymers **30**, 1191 (1969).
[8] R. Kubo, J. Phys. Soc. Jpn. **12**, 570 (1957).
[9] F. Oosawa, Biopolymers **9**, 677 (1970).
[10] A. Minakata, N. Imai, and F. Oosawa, Biopolymers **11**, 347 (1972).
[11] A. Warashina and A. Minakata, J. Chem. Phys. **58**, 4743 (1973).
[12] A. Szabo, M. Haleem, and D. Eden, J. Chem. Phys. **85**, 7472 (1986).
[13] M. Fixman, J. Chem. Phys. **72**, 5177 (1980).
[14] M. Fixman, Macromolecules **13**, 711 (1980).
[15] D. C. Rau and E. Charney, Biophys. Chem. **14**, 1 (1981).
[16] H. Washizu and K. Kikuchi, Colloids Surf., A **148**, 107 (1999).
[17] H. Washizu and K. Kikuchi, J. Phys. Chem. B **110**, 2855 (2006).
[18] K. Ito, A. Yagi, N. Ookubo, and R. Hayakawa, Macromolecules **23**, 857 (1990).
[19] A. Katchalsky, Pure Appl. Chem. **26**, 327 (1971).
[20] T. Odjik, Macromolecules **12**, 688 (1979).
[21] M. C. Murphy, I. Rasnik, W. Cheng, T. M. Lohman, and T. Ha, Biophys. J. **86**, 2530 (2004).
[22] K. Asami, A. Irimajiri, T. Hanai, N. Schiraishi, and K. Utsumi,

Biochim. Biophys. Acta **778**, 559 (1984).
[23] S. Takashima, J. Phys. Chem. **70**, 1372 (1966).
[24] M. Mandel, Mol. Phys. **4**, 489 (1961).
[25] G. S. Manning, J. Phys. Chem. **99**, 477 (1993).
[26] M. Gueron and G. Weisbuch, J. Phys. Chem. **83**, 1991 (1979).
[27] M. Gueron and G. Weisbuch, Biopolymers **19**, 353 (1980).
[28] H. Washizu, Ph.D. thesis, University of Tokyo, 2000.
[29] M. Fixman, J. Chem. Phys. **76**, 6346 (1982).
[30] M. L. Bret, J. Chem. Phys. **76**, 6243 (1982).
[31] T. Odijk, J. Polym. Sci., Polym. Symp. **15**, 477 (1977).
[32] J. Skolnick and M. Fixman, Macromolecules **10**, 944 (1977).
[33] Y. Feldman, E. Polygalov, I. Ermolina, Y. Polevaya, and B. Tsentsiper, Meas. Sci. Technol. **12**, 1355 (2001).
[34] G. Schwarz, J. Phys. Chem. **66**, 2636 (1962).
[35] J. M. Schurr, J. Phys. Chem. **68**, 2407 (1964).
[36] G. Ariel and D. Andelman, Phys. Rev. E **67**, 011805 (2003).